International Journal of Science and Research (IJSR)
ISSN (Online): 2319-7064
Index Copernicus Value (2016): 79.57 | Impact Factor (2017): 7.296

Structural Analysis of Rocket Nozzle

Mohan Banoth

Department of Mechanical Engineering, Jawaharlal Nehru Technological University College Of Engineering (JNTU CEJ), Jagital, Telangana, India

Abstract: ***A solid rocket motor nozzle is an essential component housed in the rear end of the rocket. The basic purpose of having this component is the conversion of the thermal energy into kinetic energy thereby imparting thrust to the missile. Nozzle Geometry is of paramount importance to understand the performance of a missile. The performance can be modified by changing the geometrical design, so as to achieve maximum effective velocity of the rocket. Nozzle design is a complex, multi- disciplinary and an iterative process. Aerodynamic, thermodynamic, structural and fabrication considerations are manipulated within the constraints to produce a preliminary nozzle configuration. The configuration thus produced is then rigorously analyzed for thermal and structural defects and also its contribution on the rockets overall performance. The iterative process is continued until a thermally and structurally adequate nozzle is obtained within the required rocket constraints. Two basic exit configurations are considered in the design process, contoured and conical. The contoured nozzle turns the flow so that the exhaust products exit in a more or less axial direction thereby reducing divergences losses. The conical nozzle on the other hand is considered due to its ease of fabrication. In this report the design and analysis of a contour nozzle for optimizing thrust as per the requirements and constraints is carried out. The design process is carried out as per the GVR Rao method which has now become an aerospace industry standard due to its ease of use and accuracy.***

1. Introduction to Rocket Nozzle

1.1 Introduction

A jet engine uses a nozzle to accelerate hot exhaust to supply thrust as delineated by Newton's third law of motion. The study of the high-temperature gas flow in a nozzle has led to the definition of a certain number of parameters, characteristic serve as a basis for evaluation of a rocket motor and also for comparison between different systems. So as to attain these parameters mathematically.

1.2 Atmospheric use

The best size of a jet engine nozzle to be used among the atmosphere is achieved once the exit pressure equals atmospheric pressure that decreases with altitude. For rockets movement from the world to orbit. Slight overexpansion causes a small reduction in potency, however otherwise will very little hurt.

For optimal lift-off performance, the pressure of the gases exiting nozzle should be at sea-level pressure; however, if a rocket engine is primarily designed for use at high altitudes and is only providing additional thrust to another "first stage" engine during liftoff in a multi-stage design, then designers will usually opt for an over-expanded nozzle (at sea-level) design making it more efficient at higher altitudes where the ambient presser is lower. This was the technique used on the area shuttle's main engines.

1.3 Vacuum use

This was the technique used on the world shuttle's main engines that spent most of their powered flight in near-vacuum whereas the shuttle's two solid rocket boosters provided the majority of the ascension thrust.

1.4 Optimum shape

The shape of the nozzle additionally with modesty affects however with efficiency the enlargement of the exhaust gases is regenerate into linear motion. The only nozzle form could be a ~12° cone half-angle that is regarding 97 economical. Smaller angles offer terribly slightly higher potency; larger angles offer lower efficiency. They are wide used on launch vehicles and alternative rockets wherever weight is at a premium.

1.5 Advanced designs

A number of additional subtle styles are projected for altitude compensation and alternative uses.

Nozzles with A part boundary include:
a) The Expansion-Deflection Nozzle
b) The Plug Nozzle
c) The Aero spike Nozzle
d) Single enlargement Ramp Nozzle (SERN)

C-D nozzles are radial out-flow nozzles with the flow deflected by a center penile.

Controlled nozzles:
a) The increasing Nozzle,
b) Bell nozzles with a removable insert and
c) The Stepped nozzles or Dual-bell nozzles.

These square measure usually terribly like bell nozzles however.

Dual-mode nozzles include:
a) The dual-expander nozzle and
b) The dual-throat nozzle.

They would once more enable multiple propellants to be used (such as RP-1) more increasing thrust.

India's PSLV calls its design 'Secondary Injection Thrust Vector Control System'; a jet engine uses a nozzle to accelerate hot exhaust to provide thrust as delineated by Newton's third law of motion.

A nozzle could be a comparatively straightforward device, simply a specially formed tube hot gases flow. During a C-D rocket nozzle.

2. Review of Literature

The length and therefore the exit space area unit famed of the nozzle so as to urge a fascinating thrust. First the exit conditions are defined and after that only the coordinates are found by using the MOC method that would meet the desired exit conditions. Since there's a awfully high rate gift within the exhaust gases and there are finite reaction rates that are gift which build the method of finding the coordinates of nozzle. George P. Sutton and Osca Biblarz. "Rocket Propulsion Elements, a Wiley-Interscience Publication. The method of coming up with the exhaust nozzle contour for optimum thrust by variational strategies. However, an answer that's shock-free isn't attainable by these strategies. It is obtained for the case of equilibrium and frozen chemistry. D.R. Bartz "Turbulent Boundary Layer Heat Transfer from Rapidly Accelerating Flow of Rocket Combustion Gases and of Heated Air". Jet Propulsion Laboratory. Many nozzle contours are designed mistreatment this approach and also the corresponding vacuum performance is given.

M. Barrere, and J. Vandenkerckhove, "Rocket Propulsion", Elsevier Publishing Company, Amsterdam, 1960. The developments of the supersonic jets from these nozzles are examined in under expanded, perfectly expanded and over expanded conditions.

As a consequence, there's no absence of shock noise at or close to the planning condition. These nozzles manufacture shock cells 9%-25% shorter than cells from a comparable swimmingly contoured nozzle. The Experimental/Numerical project sponsored by the Swedish Defense Materiel Administration (FMV) to apply flow control techniques to reduce the noise from high performance military aircraft such as the Saab Gripes. At University of metropolis chevrons and trailing-edge fluidic injection were tested and compared with secondary flow simulating forward flight. At Chalmers University identical conditions were simulated with giant Eddy Simulation and G. R. Kirchhoff methodology.

G.V.R. Rao method, Exhaust Nozzle Contour for Optimization thrust, jet propulsion, June, 1958. The problem of high-speed compressible flow through focused round shape nozzles is studied computationally mistreatment the final purpose ANSYS Fluent. A pressure-based coupled solver formulation with weighted second-order central-upwind spatial discrimination is applied to calculate the numerical solutions. 15˚, 25˚ and 40˚ axis symmetric conical nozzles and a reference nozzle with a circular arc cross section are considered.

3. Nozzle Theory

3.1 Introduction

The basic parameters function a basis for analysis of a rocket motor and conjointly for comparison between totally different systems. So as to make these parameters mathematically, it's necessary to form U.S.E of a sufficiently easy model showing varied phenomena considered; this leads us to form various assumptions, the validity of that should be even.

3.1 Assumptions and fundamental equations

Allow us to contemplate a perfect rocket motor assumption.

1) The combustion gases are homogeneous.

The combustion gases law:

$$p = \rho RT \tag{3.1}$$
$$P/(\rho) = RT \tag{3.1.1}$$

Where

R is the Specific gas constant ($R=R_0$ /m, R_0 being the universal gas constant and m the molecular mass)

2) The particular heats of the gas don't vary with temperature and pressure.
3) The flow is meant to be one-dimensional, steady and physical property.

It states that the decrease in enthalpy in the nozzle is equal to increase in kinetic energy. Indicating the initial state within the chamber by the subscript c, it is written:

$$\frac{V_c^2}{2} + c_p T_c = \frac{V^2}{2} + c_p T \tag{3.2}$$

This relation expresses the fact that the total or stagnation temperature τ_{tot} remains constant. Stagnation temperature is outlined because the temperature obtained by decelerating the flow to rest through an adiabatic transformation with or while not losses.

$$T_{tot} = \tau + (V^2/(2C_P)) = \tau\,(1 + (\gamma-1)/2\ M^2) \tag{3.3}$$

From equation (3.2), a limiting rate VL will be outlined it's the speed that might be reached by increasing isentropically into vacuum:

$$V_L = \sqrt{2 c_p \tau_{tot}} \tag{3.4}$$

The second fundamental equation is that of continuity

$$m^{\cdot} = \rho V A \tag{3.5}$$

Where

A is that the space of section thought-about. Finally the physical property flows square measure characterized by the relationship:

$$p\rho^{-\gamma} = constant$$

From that we tend to deduce:

$$\frac{T}{T_c} = \left(\frac{p}{p_c}\right)^{\frac{\gamma-1}{\gamma}} = \left(\frac{\rho}{\rho_0}\right)^{\gamma-1} \tag{3.6}$$

Total pressure is sometimes used and is defined as the pressure obtained by decelerating the flow to rest through an isentropic transformation.

$$p_{tot} = p\left(\frac{\tau_{tot}}{\tau}\right)^{\frac{\gamma}{\gamma-1}} = p\left(1 + \frac{V^2}{2c_p\tau}\right)^{\frac{\gamma}{\gamma-1}} = p\left(1 + \frac{\gamma-1}{2}\ M^2\right)^{\frac{\gamma}{\gamma-1}} \tag{3.7}$$

3.2 Aerodynamic choking of nozzle

If the initial velocity V_C is zero, one can easily deduce from equations (3.2), (3. 5) and (3.6), the link that links the mass flow per unit space (m/A)˙ with the upstream conditions and also the reciprocal of the growth ratio; it is:

$$\frac{\dot{m}}{A} = \sqrt{\frac{2\gamma}{\gamma-1} p_c \rho_c [(\frac{p}{p_c})^{\frac{2}{\gamma}} - (\frac{p}{p_c})^{\frac{\gamma+1}{\gamma}}]} \qquad (3.8)$$

The 2nd member of this equation is adequate to zero once p = p_c or p = 0.

Let the subscript t indicate the crucial conditions: the crucial pressure quantitative relation is often found by golf shot capable zero the spinoff of m˙ /A with relation to p/pc, and that we get:

$$\frac{p_t}{p_c} = (\frac{2}{\gamma+1})^{\frac{\gamma}{\gamma-1}} \qquad (3.9)$$

And consequently

$$\frac{\tau_t}{\tau_c} = \frac{2}{\gamma+1} \qquad (3.10)$$

The essential pressure magnitude relation pt/pc so separates 2 sorts of nozzles.

If (pe/pc) ≥ (pt/pc), the nozzle designed to provide a given mass flow ṁ is entirely

If (pe/pc) &let; (pt/pc), the nozzle designed to drop the pressure of flow(m)˙to close should be initial of decreasing section, Such a nozzle is termed a Convergent-Divergent or First State Laval Nozzle.

At the throat, it is often without delay;

$$V_t = \sqrt{\gamma \frac{p_t}{\rho_t}} = \sqrt{\gamma R \tau_t} = a_t \qquad (3.11)$$

The nozzle is claimed to be saturated or obstructed and its mass flow is entirely. Relations (3.9), (3.10) and (3.11) stay valid for physical property nozzles during which the body of water speed isn't zero.

3.3 Mass flow through a nozzle

The mass flow m˙through a nozzle , expressed as a operate of the measurable existing within the combustion chamber (pc, τ_c) and of the throat space At, may be determined as follows.

$$\dot{m} = \rho_t a_t A_t = \rho_c A_c \left(\frac{a_t}{a_c}\right)\left(\frac{\rho_t}{\rho_c}\right) A_t \qquad (3.12)$$

By neglecting the velocity V_C at the nozzle inlet, quite justified relations (3.10) and (3.11) give as:

$$\frac{a_t}{a_c} = (\frac{\tau_t}{\tau_c})^{\frac{1}{2}} = (\frac{2}{\gamma+1})^{\frac{1}{2}} \qquad (3.13)$$

Now, isentropic and relations (6), (10) lead to:

$$\frac{\rho_t}{\rho_c} = (\frac{\tau_t}{\tau_c})^{\frac{1}{\gamma-1}} = (\frac{2}{\gamma+1})^{\frac{1}{\gamma-1}} \qquad (3.14)$$

Thus, by eliminating ρ_t/ρ_c and a_t/a_c, we get:

$$\dot{m} = \rho_c a_c A_t \, (\frac{2}{\gamma+1})^{\frac{1}{\gamma-1}+\frac{1}{2}} \qquad (3.15)$$

By replacing a_c by the expression:

$$a_c = \sqrt{\gamma R \tau_c} \qquad (3.16)$$

By eliminating ρ_c by means of the perfect gas law (3.1.1) and by plase:

$$\Gamma = \sqrt{\gamma} \, (\frac{2}{\gamma+1})^{\frac{\gamma+1}{2(\gamma-1)}} \qquad (3.17)$$

We ultimately get:

$$\dot{m} = \Gamma \frac{p_c A_t}{\sqrt{R\tau_c}} \qquad (3.18)$$

The mass flow m˙may be expressed as a operate of the limiting rate VL given by(3.4)

$$\dot{m} = \Gamma \frac{2\gamma}{\gamma-1} \frac{p_c A_t}{V_L} \qquad (3.19)$$

Equation (3.18) is very often used in a particularly simple form by introducing the mass flow factor C_D or the characteristic velocity c^* defined as follows:

$$C_D = \frac{1}{c^*} = \frac{\Gamma}{\sqrt{R\tau_c}} \qquad (3.20)$$

Equation (12) can be written:

$$\dot{m} = C_D p_c A_t = \frac{p_c A_t}{c^*} \qquad (3.21)$$

Nozzle exhaust velocity

Velocity V_c being assumed negligible and, taking into assount relation (3.6) which characteristics isentropic processes, the energy qquation (3.2) can be given.

$$\frac{V_c^2}{2} = c_p\,(\tau_c - \tau_e) = c_p \tau_c [1 - (\frac{p_e}{p_c})^{\frac{\gamma-1}{\gamma}}] \qquad (3.22)$$

As we realize that:

$$\gamma = \frac{c_p}{c_v} \text{ and } R = c_p - c_v = \frac{R_0}{m}$$

Where R0 is that the universal R:

$$2c_p \tau_c = \frac{2\gamma}{\gamma-1} R\tau_c = \frac{2\gamma}{\gamma-1} \frac{R_0}{m} \tau_c \qquad (3.23)$$

Thus:

$$V_c = \sqrt{\frac{2\gamma}{\gamma-1} \frac{R_0}{m} \tau_c \, [1 - (\frac{p_e}{p_c})^{\frac{\gamma-1}{\gamma}}]} \qquad (3.26)$$

Introducing the limiting speed VL outlined by equation (4) we are able to write relation (3.26) in significantly easy form

$$V_e = V_L \sqrt{1 - (\frac{p_e}{p_c})^{\frac{\gamma-1}{\gamma}}} \qquad (3.27)$$

Equation (3.26) brings out the different variables that inflence the exhaust velocity V_c they are the pressure ratio p_c/p_e, the initial temperature in the chamber τ_c, the molecular weight m of the gases, and their specific heat ratio γ.

(A) Increasing the chamber presure, however, reduces. Despite its favourable influence, pressure increase is limited by practical design considerations

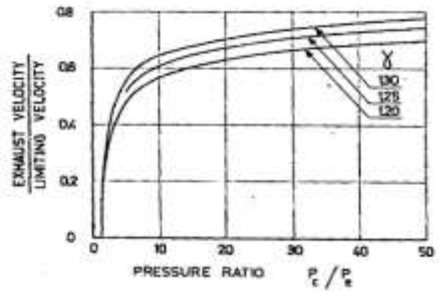

Figure 3.1: Variation of the ratio Ve/VL as a function of pressure ratio pc/pe for several values of γ

(B) Velocity V_e varies as the square root of the combustion temperature τ_e; it is thus describle to choose propellants that give a high value of τ_c. This limits set practically at between 2750 to 3500 degrees Kelvin. Only a few chemical reactions give higher temperatures at the price of considerable difficulties (for instance the reaction fluorine-hydrogen gives τ_c> 5000°K).

(C) This molecular weight m of the reaction are be possible.

(D) The specific heat ratio γ both factors of equation (3.27) .

The first corresponds to the initial enthlpy C_p τ_c, i.e. to the limiting rate, it decreases once γ will increase (Figure 3.2)

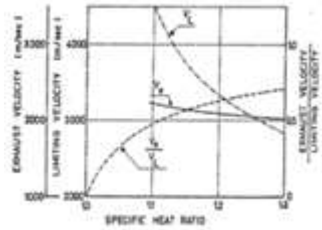

Figure 3.2: Variation of the exit velocity Ve , of the limiting velocity VL and of the ratio Ve/VL as functions of the specific heat ratio in the case: pc/pe = 20, and m=25

The second factor,

$$\sqrt{1-\left(\frac{p_e}{p_c}\right)^{\frac{\gamma-1}{\gamma}}} \tag{3.28}$$

Corresponds to the expansion and increase together with γ).

The real process lies in between the so-called "FROZEN FLOW" in which the composition has no time to vary and the so-called "EQUILIBRIUM FLOW" in which physical and chemical equilibrium exists at all times.

Equation (16) will be employed in a very easy kind by a parameter

$$\dot{C_F} = \Gamma\sqrt{\frac{2\gamma}{\gamma-1}\left[1-\left(\frac{p_e}{p_c}\right)^{\frac{\gamma-1}{\gamma}}\right]} \tag{3.29}$$

Equation (3.15) can be written:

$$V_e = c^*\dot{C_F} \tag{3.30}$$

Figure 3.3 represents $\dot{C_F}$ as a function of p_c/p_e for five values of γ. Equation (3.30) terribly is incredibly typically used as a result of it results in very straightforward expression of the thrust.

3.4 Area ratio (a_e/a_t)

Indeed, continuity of the mass between the throat and exit space is written:

$$\rho_e V_e A_e = \rho_t V_t A_t \tag{3.31}$$

And by mistreatment a similar transformations as with in the preceding sections

$$\frac{A_e}{A_t} = \frac{\rho_t V_t}{\rho_e V_e}\frac{\rho_t a_t \rho_c a_c}{\rho_e a_e \rho_e^{\circ} V_e} = \Gamma\left(\frac{p_c}{p_e}\right)^{\frac{1}{\gamma}}\frac{\sqrt{R\tau_c}}{V_e} \tag{3.32}$$

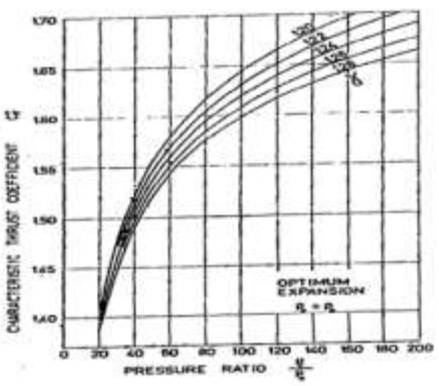

Figure 3.3: Variation of the characteristic thrust coefficient as a function of the pressure ratio pc/pe, for several values of.

In above relation, V_e can be replaced by its expression as given by equation (3.26), os that:

$$\frac{A_e}{A_t} = \frac{\Gamma}{\left(\frac{p_e}{p_c}\right)^{\frac{1}{\gamma}}\sqrt{\frac{2\gamma}{\gamma-1}\left[1-\left(\frac{p_e}{p_c}\right)^{\frac{\gamma-1}{\gamma}}\right]}} = \frac{\Gamma^2}{\left(\frac{p_e}{p_c}\right)^{\frac{1}{\gamma}}\dot{C_F}} \tag{3.33}$$

Also, conversely the ratio p_e/p_c is completely determined when A_e/A_t is fixed, as long as no flow separation takes place within the divergent.

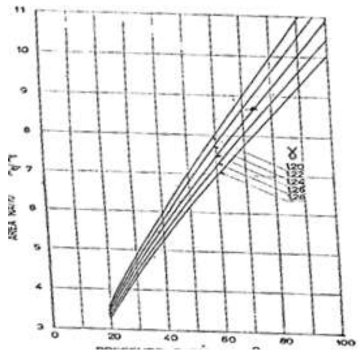

Figure 3.4: Variation of the area ratio Ae/At as a function of pressure ratio pc/pe, for several values

Figures 3.4 (3.3) and 3.5 give the values of the area ratio A_e/A_t as a function of pressure ratio p_c/p_e, for different values of γ. $(p_e/p_c)^{\frac{1}{\gamma}}$ can easily readily obtained from:

$$\left(\frac{p_e}{p_c}\right)^{\frac{1}{\gamma}} = \frac{\frac{p_e}{p_c}}{\left(\frac{p_e}{p_c}\right)^{\frac{\gamma-1}{\gamma}}}$$

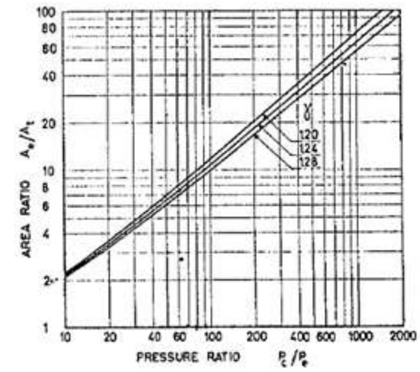

Figure 3.5: Variation of the area ratio A_e/A_t as a function of pressure ratio p_c/p_e, for several values of γ.

3.5 Thrust and thrust coefficient

The flow of the propellant gases or the momentum flux-out causes the thrust force on the rocket structure plane of the nozzle could also be totally different from the close pressure.

$$F = \dot{m}v_2 + (p_2 - p_3)A_2 \tag{3.35}$$

Values calculated for optimum operative conditions (p2=p3) for given values of p1,k, and A_2/A_t, the subsequent expressions could also be used. For the thrust,

$$F = F_{opt} + p_1 A_t\left(\frac{p_2}{p_1} - \frac{p_3}{p_1}\right)\frac{A_2}{A_t} \tag{3.36}$$

For specific impulse,

$$I_s = (I_S)_{opt} + \frac{c^*\epsilon}{g_0}\left(\frac{p_2}{p_1} - \frac{p_3}{p_1}\right) \tag{3.37}$$

If, as an example, the particular impulse for a replacement exit pressure p_2 such as a replacement space quantitative relation A_2/A_t is to be calculated, the on top of relations could also be used.

Equation 3.3 can be modifying and substituting v_2, v_t and V_t.

$$F = \frac{A_t v_t v_2}{V_t} + (p_2 - p_3)A_2$$

$$F = A_t p_1 \sqrt{\frac{2k^2}{k-1}\left(\frac{2}{k+1}\right)^{(k+1)/(k-1)}\left[1-\left(\frac{p_2}{p_1}\right)^{(k-1)/k}\right]} + (p_2 - p_3)A_2 \quad (3.38)$$

The pressure quantitative relation the nozzle [p1/p$_2$], heat quantitative relation k, and of the pressure thrust. The thrust constant C_F is outlined because the thrust divided by the chamber pressure p_1 and also the throat space elevation

$$C_F = \frac{{v_2}^2 A_2}{p_1 A_t V_2} + \frac{p_2}{p_1}\frac{A_2}{A_t} - \frac{p_3}{p_1}\frac{A_2}{A_t}$$

$$C_F = A_t p_1 \sqrt{\frac{2k^2}{k-1}\left(\frac{2}{k+1}\right)^{(k+1)/(k-1)}\left[1-\left(\frac{p_2}{p_1}\right)^{(k-1)/k}\right]}\frac{p_2 - p_3}{p_1}\frac{A_2}{A_t} \quad (3.39)$$

The thrust constant C_F could gas property k,
This peak price is thought because the optimum thrust constant

$$F = C_F A_t p_1 \quad (3.40)$$

The above equation can be solved for C_F and provides the relation for determining the thrust coefficient experimentally.

4. Materials and Methods

Materials used

The solid propellant rocket nozzle mainly uses four different composites namely Aluminum 7075, Silica-Phenolic, Carbon Phenolic, Graphite.

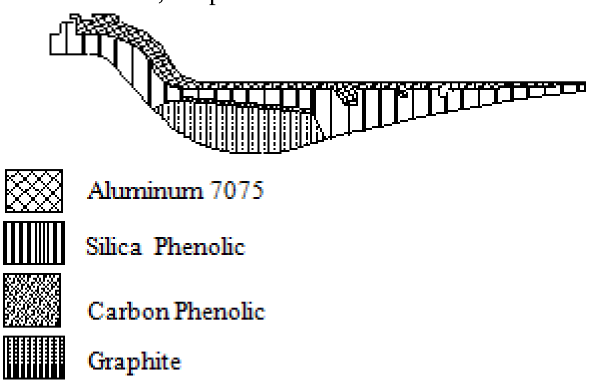

Figure 4.1 Material Representation of nozzle

4.1 Aluminum 7075

Aluminum alloy 7075 is AN aluminum alloy. It has lower resistance to corrosion than several alternative Al alloys; however has considerably higher corrosion resistance than the 2000 alloys. 7075 aluminum alloy's composition roughly includes five.6–6.1% zinc, 2.1–2.5% magnesium, 1.2–1.6% copper, and less than a half percent of silicon, iron, manganese, titanium, chromium, and other metals.

Thermal conductivity : 177 W/m K
Specific heat : 890 J/Kg
Density : 2700 Kg/ m3
Ultimate tensile strength : 42.9 MPa
Young's modulus : 7378 MPa
Poisson's ratio : 0.33

Table 4.1: The Variation of Thermal Conductivity and Specific with respect to Temperature

Temperature(k)	300	1000	1500	2000	2500	3000
Thermal Conductivity (W/mk)	0.5424	0.5693	1.875	5.2615	11.619	1443
Specific heat(J/Kgk)	1087.1	1336.9	1426.8	1443	1443	1443

4.2 Silica phenolic

Density : 1350 Kg/ m3
Ultimate tensile Strength : 9 MPa
Young's modulus : 1700 MPa
Poisson's ratio : 0.28

4.3 Carbon phenolic

Ablative materials are commonly used. Because of the extraordinarily harsh atmosphere within which these materials operate, they're worn throughout motor firing with a ensuing nominal performance reduction. The objective of the present work is to study the thermo chemical erosion behavior of carbon-phenolic material in solid rocket motor nozzles. The adopted approach relies on a validated full Navier-stokrs flow solver coupled with a thermo chemical ablation model, which takes into account finite-rate heterogeneous chemical reactions at the nozzle surface, rate of diffusion of the species through the boundary layer, pyrolysis gas and char-oxidation product species injection in the boundary layer heat conduction inside the nozzle material, and variable multispecies thermo physical properties.

Thermal Conductivity : 0.56 W/m K
Specific heat : 0.177 J/Kg k
Density : 1350 Kg/ m3
Ultimate tensile Strength : 10 MPa
Young's modulus : 900 MPa
Poisson's ratio : 0.25

4.4 Graphite

Graphite archaically stated as plum bago, could be a crystalline kind of carbon, a semimetal, a native component mineral, and one in all the allotropes of carbon. Carbon is that the most stable kind of carbon underneath normal conditions. Carbon happens in metamorphic rocks as results of the reduction of matter carbon compounds throughout geologic process. It conjointly happens in igneous rocks and in meteorites. In meteorites it happens with toilet and salt minerals.

Density : 1900 Kg/ m3
Ultimate tensile Strength : 10.5 MPa
Young's modulus : 1180 MPa
Poisson's ratio : 0.3

Table 4.2: The Variation of Thermal Conductivity and Specific Heat with respect to Temperature

Temperature(k)	300	1500	2000	2500	3000
Thermal conductivity(W/k)	106.41	40.049	35.064	36.078	38.091
Specific heat(J/Kgk)	800	1950	2050	2050	2050

5. Contour Nozzle Design

Different methods have been proposed to design the profile of a nozzle. Method of characteristics and G.V.R. Rao approximation method are the different methods that are discussed below.

5.1 Method of characteristics

The physical conditions of a two-dimensional, steady, isentropic, irrigational flow are often expressed mathematically by the nonlinear equation. The tactic of characteristics was initial applied to supersonic flows by Prandtl and Busemann in 1929 and has been abundant used since. This methodology supersonic nozzle style created the technique additional accessible to engineers:-

1) Contraction half, subsonic
2) The throat region, wherever the flow accelerates from high subsonic to low subsonic speeds.
3) The initial enlargement region, wherever the slope of the counter will increase up to its most worth the straightening or "Bushman" region in which the processor area increases but the wall slope decreases to 0. 5.

5.2 Importance of g.v.r rao method

Future house exploration would force increasing payload. Therefore, Optimizing the performance of finite length nozzles is often accomplished exploitation AN in pasty core flow and a physical phenomenon displacement. G.V.R. Rao developed a technique that optimizes a rocket nozzle contour for a given length or enlargement quantitative relation such most thrust is achieved. Rao's technique was supported the idea of in pasty physical property flow.

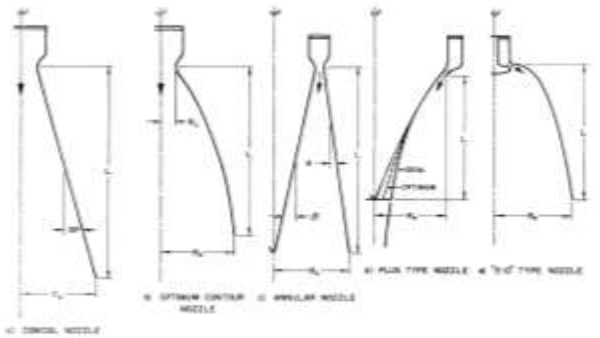

Figure 5.1: Main features of various types of nozzles

In the figure F.1, we can see that the different types of nozzle can be optimized by using the Rao's method.

Basically two types of nozzle contours have been considered- conical and contoured. In this thesis, the look procedure followed to style a contour nozzle is delineating. The difference between θ_e and θ_m is 12^0. The convex or contour nozzle is maybe the foremost common nozzle form nowadays.

The enlargement within the supersonic bell nozzle is additional economical than during a easy straight cone of comparable space quantitative relation and length, as explained later during this section. For the past many decades most of the nozzles are bell formed. Between the inflection points I and also the nozzle exit E the flow space remains. The angle at the exit θ_e is little, typically but 10°. Once the gas flow is turned within the wrong way (between points I and E) oblique compression waves can occur. These compression waves area unit skinny surfaces wherever the flow undergoes a gentle shock, the flow is turned, and also the speed is truly reduced slightly. It's attainable to balance the oblique growth waves with the oblique compression waves and minimize the energy loss.

A throat approach radius of $1.5r_t$ and a throat expansion radius of 0.4 rats were used.

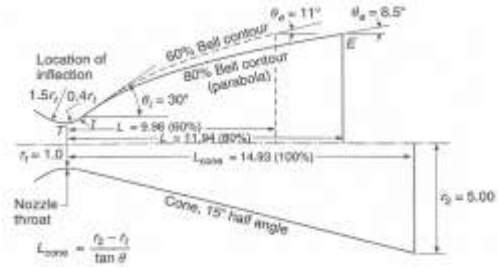

Figure 5.2: Comparison sketches of nozzle inner wall surfaces for 15 degrees conical nozzle, an 80% length bell nozzle, at 60% length bell nozzle, all at an area ratio of 25.

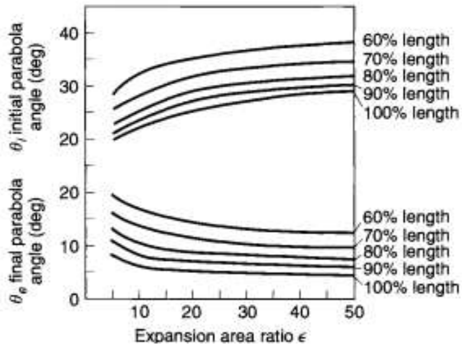

Figure 5.3: Graph showing the variation of the area ratio with the final and initial angle of inflection.

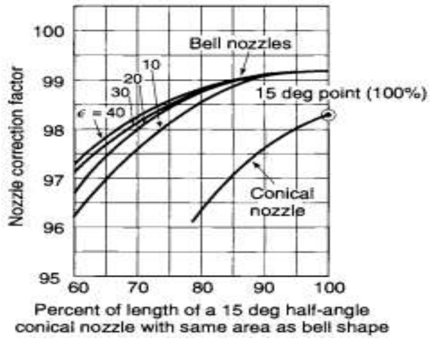

Figure 5.4: Graph showing the variation of the nozzle correction factor with the percentage of length of a 15 deg half angle conical nozzle with same area as bell shape.

Table 5.1: Data on Several Bell Shaped Nozzles

Area Ratio	10	25	50
Cone (15° Half Angle)			
Length (100%)	8.07	14.93	22.66
Correction Factor λ	0.9829	0.9829	0.9829
80% Bella Contour			
Length [a]	6.45	11.94	18.12
Correction Factor λ	0.985	0.987	0.988
Approximate half angle at inflection point & exit (degrees)	25/10	30/8	32/7.5

60% Bella Contour Length [a]	4.84	9.96	13.59
Correction Factor λ	0.961	0.968	0.974
Approximate half angle at inflection point & exit (degrees)	32.5/17	36/14	39/18
[a] The Length is given in dimensionless form as a multiple of the throat radius, which is one.			

The above table shows data for parabolas developed from this figure, which allow the reader to apply this method and check the results. The reduced length is a very important profit, associated it's sometimes mirrored in an improvement of the vehicle mass magnitude relation. The table and Fig.5.2, 5.3, 5.4 show that bell nozzles (75 to 85% length) are just as efficient as or slightly more efficient than a longer 15 ° conical nozzle (100% length) at the same area ratio. For shorter nozzles (below seventieth equivalent length) the energy losses thanks to internal oblique shock waves become substantial and such short nozzles aren't usually used these days.

The erosion will become acceptable. Typical solid rocket motors flying these days have values of inflection angles between twenty and twenty six ° and turn-back angles of 10° to 15°. In comparison, current liquid rocket engines without entrained particles have inflection angles between 27 and 50° and turn-back angles of between 15 and 30°.

Therefore the performance improvement caused by employing a bulging nozzle (high worth of correction factor) is somewhat lower in solid rocket motors with solid particles within the exhaust. The best bulging nozzle (minimum loss) is long; adore a conic nozzle of maybe 10○ to 12°. It's concerning identical length as a full-length aero spike nozzle.

5.3 Designing of contour by GVR Rao method

5.3.1 Overview

The wall contour for the nozzle divergent portion is designed to yield maximum thrust based on G.V.R. Rao procedure.

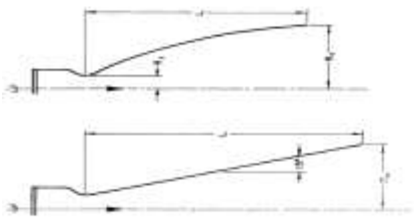

Figure 5.5: Difference between the Contour Nozzle and a Conical Nozzle

5.3.2 Analytical procedure to find θ_m and θ_e

The throat region is delineated by 2 circular arcs – a circular arc of radius two times throat radius (Yt) on the convergent aspect and another circular arc of radius up to 1.2 Y_t on the divergent side . With these initial throat conditior a .V.R Rao gives parametric curves for a nozzle having a certain area ratio A_e/A_m S_t and length ratio L/Y_t. G.V.R. Rao method has also derived an equation to calculate the value of θ at the nozzle exit. The given by

$$Sin(2\theta) = \frac{(p-p_a)}{0.5\rho w^2}\cot\alpha \qquad (5.1)$$

Where,
p = Nozzle exit pressure
P_a = Ambient pressure
ρ = Density of gases
W = Velocity of gases

$$\alpha = \sin^{-1}\left(\frac{1}{M}\right) \qquad (5.2)$$

Where,
M = Mach number flow at the exit

$$w^2 = \gamma RTM^2 \qquad (5.3)$$

For exit conditions the worth of pa are one, therefore the exit angle may be determined by following formula.

$$\sin 2\theta = \frac{(p-1)}{0.5\rho w^2}\cot\alpha \qquad (5.4)$$

For vacuum condition the value of p_a will be 0. the formula becomes

$$Sin(2\theta) = \frac{(p)}{0.5\rho w^2}\cot\alpha \qquad (5.5)$$

5.3.3 Graphical approach to find θ_m and θ_e

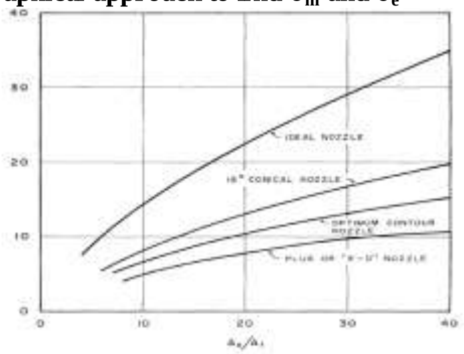

Figure 5.6: Length Comparison of Various types of Nozzles

Diagrammatically the worth of θ at the nozzle exit is found by determinative the point of L/y_t and ye/y_t given 2 equations once it's taken on the graph.

$$\frac{L}{y_t} = constant$$

$$\frac{Y_e}{Y_t} = \text{constant}$$

For the present nozzle design the following nozzle dimensions are used.
Throat diameter = d_t
Throat radius $r_t = y_t$
Exit radius $r_e = y_e$
Exit diameter = d_e
Length of divergence = L

Thus from the on top of graph the θe and θm are often obtained. It are often determined that worth the worth of θe square measure in shut agreement compared to the value that is analytically calculated for water level. The circular arc at the throat and the parabolic divergent contour intersect tangentially which defines point M. This point is the values of θm and θe

5.3.4 Calculation for parabolic equation

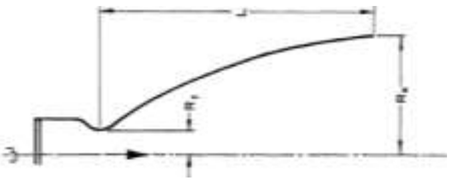

Figure 5.7: Optimum Contour Nozzle

Let the parabola be described by the equation $y = ax^2 + bx + c$ where x is from inflection point M to the nozzle exit. The boundary condition is:

$$y = ax^2 + bx + c \tag{5.6}$$

$$\text{At } \; x = 0,\; \frac{dy}{dx} = \tan\theta_m$$

Thus the worth of b may be determined by mistreatment equation 2ax+b=tan θ_m

$$x = 0, y = c = yt$$

$$b = \tan\theta_m \tag{5.7}$$

Let the value of the distance of the inflection point at the exit be x_i

At the exit inflection point the boundary conditions are:

$$x = xt \; and \; \frac{dy}{dx} = \tan\theta_e$$

$$a = \frac{\tan\theta_m - \tan\theta_e}{2xt} \tag{5.8}$$

Thus the parabolic equation will be obtained by substituting the values of a, b and c:

$$y = \frac{\tan\theta_m - \tan\theta_e}{2xt} x^2 + \tan\theta_m x + y_t \tag{5.9}$$

Thus the value of y co-ordinates can be found by substituting the value of x in the above equation by marching towards left along the nozzle length.

5.4 Casing design

The casing style of a contour nozzle consists of the subsequent steps.

1) Calculation for the value of θ_m and θ_e
2) Determining the parabolic equation
3) Calculation of the co-ordinates of the divergent section of the nozzle by mat-lab program
4) Profile design
5) Calculation of the liner thickness
6) Modeling in CAD

5.4.1 Calculation for the value of θ_m and θ_e

According to the given problem statement, the following input parameters are taken under consideration

Table 5.2: Input parameters

Thrust	2600 Kgf
Action time	10 sec
I_{sp}	246 sec
γ	1.1906
Pe	2.4 Ksc
A_e/A_t	7
Pa	1.032 Ksc
Pc	100 Ksc
c^*	1525 m/sec

$$C_F = \Gamma \sqrt{\frac{2\gamma}{\gamma-1}\left(1-\left(\frac{P_e}{P_c}\right)^{\frac{\gamma-1}{\gamma}}\right)} + \frac{A_e}{A_t}\left[\frac{P_e}{P_c} - \frac{P_a}{P_c}\right] \tag{5.10}$$

$$\Gamma = \sqrt{\gamma}\left(\frac{2}{\gamma+1}\right)^{\frac{\gamma+1}{2(\gamma-1)}} \tag{5.11}$$

$$I_{sp\;req} = \frac{C * C_F \eta}{g}$$

$$Propellant\ mass\ (Mp) = \frac{total\ impulse}{I_{sp}}$$

$$Total\ impulse = thrust \times time$$

$$Throat\ diameter\ (D_t) = \sqrt{\frac{\dot{m}_p \times C^* \times 4}{P_c \times \pi}}$$

The calculation of the throat diameter of the given rocket motor was disbursed as follows:

$$\Gamma = \sqrt{1.1906}\left(\frac{2}{1.1906+1}\right)^{\frac{1.1906+1}{2(1.1906-1)}}$$

$$\Gamma = 0.646$$

$$C_F = 0.646 \sqrt{\frac{2 \times 1.1906}{1.1906 - 1}\left(1 - \left(\frac{2.4}{100}\right)^{\frac{1.1906-1}{1.1906}}\right) + 7 \times \left[\frac{2.4}{100} - \frac{1.032}{100}\right]}$$

$$C_F = 1.545$$

$$I_{sp}\ req = \frac{1525 * 1.545 * 0.97}{9.81}$$

$$I_{sp}\ req = 232.97056\ seconds$$

$$Propellant\ mass\ (Mp) = \frac{2600 * 10}{232.97056}$$

$$Propellant\ mass\ (Mp) = 111.602\ kgs$$

$$Mass\ flow\ rate = \frac{111.602}{9}\ kgs/seconds$$

$$Mass\ flow\ rate = 12.400 kgs\ /sec$$

$$Throat\ diameter\ (D_t) = \sqrt{\frac{12.400 \times 1525 \times 4}{100 \times 98100 \times \pi}}$$

$$Throat\ diameter\ (D_t) = 49.54mm \cong 50mm$$

$$Exit\ diameter (D_e) = \sqrt{\frac{Ae}{At}} * Dt$$

$$Exit\ diameter (D_e) = \sqrt{7} * 68.481mm$$

$$Exit\ diameter (D_e) = 132.287mm$$

$$Throat\ radius\ (y_t) = 25mm$$

$$Exit\ radius (r_t) = 66.143\ mm$$

The throat region is delineate by 2 circular arcs – a circular arc of radius a pair of times throat radius (Yt) on the focused aspect and another circular arc of radius capable 1.2Y_t on the divergent side. With these initial throat conditions, G.V.R Rao gives parametric curves for a nozzle having a certain area ratio A_e/A_t and length ratio L/Y_t.

G.V.R. Rao methodology has additionally derived an equation to calculate the worth of at the nozzle exit. This is often given by

$$\sin 2\theta = \frac{(p - pa)}{0.5\rho w^2}\cot\alpha \tag{5.12}$$

Where,

p = Nozzle exit pressure=2.4ksc
P_a = Ambient pressure=1.0332ksc
ρ = Density of gases
W = Velocity of gases

$$\alpha = \sin^{-1}\left(\frac{1}{M}\right) \tag{5.13}$$

$$\alpha = \sin^{-1}\left(\frac{1}{3.05}\right)$$

$$\alpha = 19.14$$

Where,
M = Mach number of the flow at the exit

$$W^2 = \gamma R T M^2$$

$$W^2 = 1.1906 \times \frac{8.314}{25.14} \times$$

1495 α $(3.05)^2$

$$W^2 = 5480187$$

$$W = 2340.97$$

The density of the gas given rocket motor is determined by victimization the subsequent equation.

$$\rho = \frac{2.4 \times 98100}{330.7 \times 1495}$$

$$\rho = 0.4758 \ kg/m^3$$

For exit conditions the value of p_a will be 1, thus the exit angle can be determined by.

$$\sin 2\theta = \frac{(2.4 - 1.032)}{0.5 \times 0.4758 \times 2340.97} \cot(19.14)$$

$$\theta_m = 21^{\circ}$$

5.4.2 Determination of parabolic equation

Let the parabola be described by the equation

$$y = ax^2 + bx + c \qquad (5.14)$$

Where 'x' starts inflection 'M' nozzle exit,
The boundary conditions two measures:

$$At\ x = 0,\ \frac{dy}{dx} = \tan \theta_m$$

Thus the value of b can be determined by using equating $2ax + b = \tan \theta_m$

$$At\ x = 0, y = c = Y_t$$

$$b = \tan \theta_m$$

$$\text{b} = \tan 21$$

$$b = 0.3838$$

Let the value of the distance of the inflection point at the exit be x_i

$$a = \frac{\tan\ 9 - \tan 21}{2 \times 152.5}$$

$$a = -7 \times 10^{-4}$$

Thus the parabolic equation will be obtained by substituting values of a, b and c:

$$y = \frac{\tan\ 9 - \tan 21}{2xt} x^2 + \tan 21\, x + y_t$$

$$\text{y} = \frac{\tan 9 - \tan 21}{2 \times 152.5} x^2 + \tan 21\text{x} + 26.9921$$

$$y = -7 \times 10^{-4} + 0.3838\ x + 26.9921 \qquad (5.15)$$

Thus the value of y co-ordinates can be found by substituting the value of x in the above equation by marching towards left along the nozzle length.

5.4.2 Calculation of co-ordinates of divergent section of nozzle by mat-lab program

```
X_ip=input('enter x_ip')
y_ip=input('enter ')
the_m=input('enter ')
the_e=input('enter ')
l=input('enter ')
area_rat=input('enter ')
thr_d=input('enter ')
PI=3.14159265
b=tan(the_m*PI/180)
a=(tan(the_e*PI/180)-tan(the_m*PI/180))/(l*2)
c=y_ip
exit_r=sqrt(area_rat)*thr_d/2
x=0
y=0
s=0

while y<exit_r
   x=s+x_ip
   y=a*x*x+b*x+c
   format long
   disp(x)
   disp("--")
   disp(y)
   s=s+2
end
```

5.4.3 Profile design

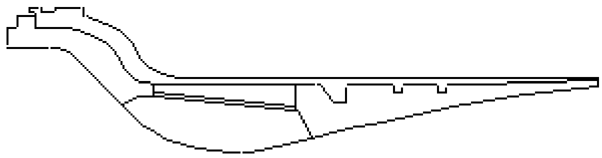

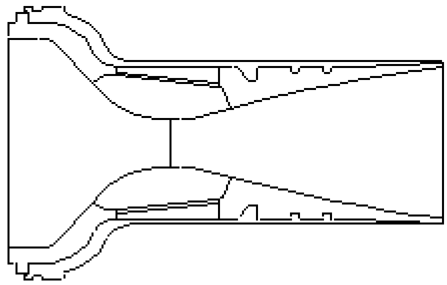

(B) 2-D Complete Nozzle

The profile design of the nozzle is done in the software design package, AutoCAD. In this design, the commands used are point, Axis line, Circle, Spline, Lines, Fillet, Offset, Trim and etc.

From there, the parabola is drawn from the point of inflection till the nozzle exit for the divergent section. For the convergent section there is no any specific method of designing method. Hence it's designed in step with the need of the length of the nozzle. The velocity of the hot gasses will accelerate from the inlet of the nozzle to the exit.

5.4.5 Calculation of the liner thickness

The calculation of the liner thickness 2 section

1) Nozzle convergent section insulation
2) Nozzle divetgent section insulation

Nozzle convergent section insulation:

For silicon dioxide phenoplast system the erosion rate measured is 0.328mm/sec for a computed heat fluxfrom the convergent section. It is zero.415mm/sec. The liner thickness erosion rate 0.415mm/sec for length of 12sec operations. additionally to the present, a char of 2mm thickness is taken into account. the ultimate liner thickness is reported by considering an element of safety of 1.5, where FOS= initial thickess/thickness eroded.

$$t_{conv} = [(9\text{sec}) \times 0.415\text{mm/sec} + 2\text{mm}] \times 1.5 = 8.535\text{mm}$$

Nozzle divergent insulation:

The maximum heat flux in the divergent section occurs at the graphite throat exit. This heat flux is calculated to be as

2000W/cm^2 fom the graph. From avalible experimental data, a maximum erosion rate of 0.225mm/sec corresponds to be calculated heat flux of 2100W/cm^2 for divergent section (at the graphite exit). This errosion rate scaled for a heat flux of 200W/cm2 is zero,214mm/sec. the thickness of the liner at the graphite throat exit in the divergent section is estimated by considering an erosion rate of 0.214mm/sec for a total firing time of 12sec motor operation. the element of safety of 1.5, where FOS= initial thickess/thickness eroded.

t_{conv} =[(9sec)×0.214mm/sec+2mm] ×1.5 = 5.889mm.

6. Thermal Analysis of Contour Nozzle

6.1 Introduction

Since, in the early days, Konstantin A. Kurbatskii1 and Angela Lestari2, "Pressure-based Coupled Numerical Approach to the Problem of Compressible Flow through Convergent Conical Nozzles" ANSYS. These walls were generally constructed of materials with negligible strength above about 1500^{o}F and had to contain gases at pressures of a few hundred pounds per square inch and temperature of 4000-5000^{0}F, the consequences of undersigned a blown-up engine; the consequence of grossly overdesigned wall protection provisions was excessive pressure drop and weight, or demands of shifts in the engine operating mixture ratio towards lower performance.

The nozzle metal like back should be protected against the big heat transfer from the interior flow. The thermal insulation style of nozzle includes evaluating liner thickness for the nozzle divergent throat and merging throat. A silicon dioxide phenolic resin nozzle liner is employed for merging and divergent of nozzle. Black lead insert is employed at the throat to cut back the erosion and maintain a gentle operative pressure.

6.2 Method of calculating the heat flux

The heat transfer to the wall is calculated by using Bartz equation.

$$hg = \left(\frac{0.026}{D^{*0.2}}\right)\left(\frac{\mu^{0.2}C_p}{P_r^{*0.6}}\right)\left(\frac{P_c g}{C^*}\right)^{0.8}\left(\frac{D^*}{r_c}\right)^{0.1}\left(\frac{A^*}{A}\right)^{0.9}\times\sigma \tag{6.1}$$

Where

$$P_r = \left(\frac{4\gamma}{9\gamma-5}\right) \tag{6.2}$$

$$\mu = 46.6\times10^{-10}\left(M^{1\frac{1}{2}}\right)(T_o R)^W \tag{6.3}$$

H_g= heat transfer coefficient
D*=Throat diameter
μ= Viscosity
C_p= Specific heat at constant pressure
P_r= Prandtl No.
P_e= Chamber pressure
g= Gravitational acceleration
C*= Characteristic velocity
r_c= Radius of curvature
A*=Area at the throat
A= Local area of cross section

$$\sigma = \frac{1}{\left[\frac{1}{2}\frac{T_w}{T_o}\left(1+\frac{\gamma-1}{2}M^2\right)+\frac{1}{2}\right]^{0.8-\frac{w}{5}}\left(1+\frac{\gamma-1}{2}M^2\right)^{\frac{w}{5}}}$$

(6.4)

Where,
W=0.6
T_o=Stagnation temperature
T_w= Wall temperature
M= Local Mach number
M^1=Molecular weight
The values of the parameters considered for the calculation of Bartz equation are

Table 6.1: Input parameters

S. No	Parameters	Values
1	Characteristic Velocity C*	1525m/sec
2	Throat Diameter D	50mm
3	Specific Heat at constant pressure C_p	1875.2J/kg K
4	Chamber Pressure P_c	100ksc
5	Equivalent throat radius of curvature r_c	50mm
6	Gamma γ	1.1906
7	Molecular Weight M^1	25.121
8	Stagnation Temperature T_o	2984K
9	Viscosity μ	0.020684pascals
10	Wall temperature for carbon phenolic system T_w	1000K

Method of calculating the heat flux

The heat transfer to the wall is calculated using Bartz equation.

H =

$$\left[\frac{0.026}{D^{*0.2}}\left(\frac{\mu^{0.2}C_p}{\Pr^{*0.6}}\right)\left(\frac{P_c g}{C*}\right)^{0.8}\left(\frac{D^*}{r_c}\right)^{0.1}\right]\times\left(\frac{A^*}{A}\right)^{0.9}\times\sigma,$$

H = H_1*H_2*H_3*H_4*H_5*σ *144*3600*5.6782,

Where,

$$H_1 = \frac{0.026}{D^{*0.2}},\ H_2 = \left(\frac{\mu^{0.2}C_p}{\Pr^{*0.6}}\right),\ H_3 = \left(\frac{P_c g}{C*}\right)^{0.8},\ H_4 = \left(\frac{D^*}{r_c}\right)^{0.1},\ H_5 = \left(\frac{A^*}{A}\right)^{0.9}$$

$$H_1 = \frac{0.026}{D^{*0.2}} = \frac{0.026}{(50)^{0.2}} = 0.0118,$$

$$H_2 = \left(\frac{\mu^{0.2}C_p}{\Pr^{*0.6}}\right),$$

We know the μ from tables

$\mu = 0.915 * 10^{-5}$ Lb/in.s,

C_p =1875.2*0.23884/1000 = 0.4479Btu/lbm.f ,

$\Pr = \frac{4r}{9r-5} = \frac{4*1.1906}{(9*1.1906-5)} = 0.8333,$

$H_2 = \frac{(9.15*10^{-6})^{0.2}*0.4479}{(0.8333)^{0.6}} = 0.04909$

$$H_3 = \left(\frac{P_c g}{C*}\right)^{0.8}$$

P_c = 100*9.81× 10^4 *1.45038× 10^{-4} = 1422.82 lbf/in^2,

$g = \frac{9.81\times1000}{304.8} = 32.185$ ft/sec^2,

C* = 1525× $\frac{1000}{304.8}$ = 5003.28 ft/sec,

$H_3 = [\frac{1422.82*32.185}{5003.28}]^{0.8} = 5.8781,$

$$H_4 = \left(\frac{D^*}{r_c}\right)^{0.1},$$

From tables we know the throat diameter

$r_c = 25$ For convergent and throat

$H_4 = [\frac{50}{25}]^{0.1} = 1.071$

$= [\frac{50}{30}]^{0.1}$

$$H_5 = \left(\frac{A^*}{A}\right)^{0.9}$$

$H_5 = [D^{*2}/D^2]$

$H_5 = [\frac{(50\text{^}2)}{(132.287)\text{^}2}]^{0.9}$

$H_5 = 0.17354$

Throat diameter (D*) =50

Where D is local and changes from entry to exit of nozzle

D = 132.287 ,

Where r is the radius of convergent divergent nozzle at each point ,

We obtained different H_5 values for different radius,

$$\sigma = \frac{1}{\left[\frac{1}{2}\frac{T_w}{T_0}\left(1+\frac{\gamma-1}{2}M^2\right)+\frac{1}{2}\right]^{0.8-\frac{w}{5}}\left(1+\frac{\gamma-1}{2}M^2\right)^{\frac{w}{5}}}$$

$$\sigma = \frac{1}{\left[\frac{1}{2}\frac{1000}{2984}\left(1+\frac{1.1906-1}{2}0.63^2\right)+\frac{1}{2}\right]^{0.8-\frac{0.6}{5}}\left(1+\frac{1.1906-1}{2}0.63^2\right)^{\frac{0.6}{5}}}$$

=1.3020

$H = H_1*H_2*H_3*H_4*H_5*144*3600*5.6782*1.3020$

H=0.01189*0.04909*5.8781*1.071*0.17354*144*3600*5.6782*1.3020

$H = 2443.9233\ W/(m^2K)$.

From tables we obtain T_w, T_o , γ , w

Mach number Varies from Entry to Exit of Nozzle So, we obtain one sigma value of each mach number Finally We obtain Variable Heat Transfer co-efficient values

Now Heat Flux,

$h_f = H(A_{diabatic\ wall} - T_{wall}) * 10\text{-}4$ w/cm2 ,

From Isentropic flows equation,

$$\frac{T_o}{T} = 1+\left(\frac{\gamma-1}{2}\right)M^2,$$

$$T = \frac{T_o}{1+\left(\frac{\gamma-1}{2}\right)M^2},$$

Where T is Adiabatic wall Temperature and for every Mach number, we obtain a different temperature

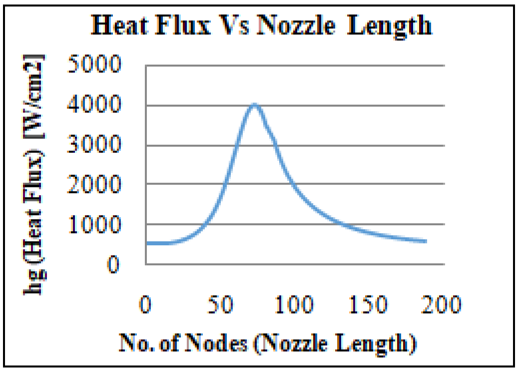

Figure 6.1: Variation of Heat Flux with Nozzle Length

By observing the above plot we can say that the value of heat transfer at the throat is more when compared with the inlet and the exit of the nozzle.

6.3 Pressure calculation

From equation (3.7) we have,

$$p_t = p_c * \left(1+\left(\frac{\gamma+1}{2}M^2\right)\right)^{\frac{\gamma}{\gamma-1}} \tag{6.5}$$

Where,

$\gamma = 1.1906$

$p_c = 1.464$

$P_t = 1.464*10\text{^}5*\left(1+\left(\frac{1.1906-1}{2}(0.63^2)\right)\right)^{\frac{1.1906}{1.1906-1}}$

$P_t = 184635.73$

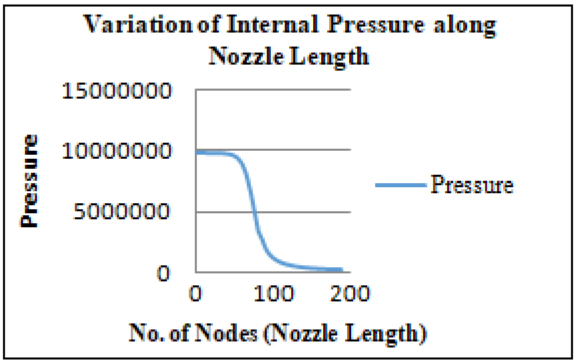

Figure 6.2: Variation of Internal Pressure along nozzle length

7. Structural Analysis

7.1 Material properties

Table 7.1: Material properties

Material	Young's Modulus (kg/mm^2)	Poisson's Ratio	Ultimate Tensile Strength (kg/mm^2)
Aluminum 7075	7378	0.33	42.9
Silica Phenolic	1700	0.28	9
Carbon Phenolic	900	0.25	10
Graphite	1180	0.3	10.5

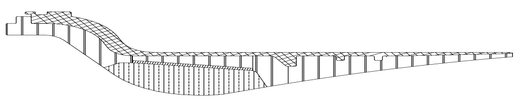

Figure 7.1: Material Representation of Nozzle

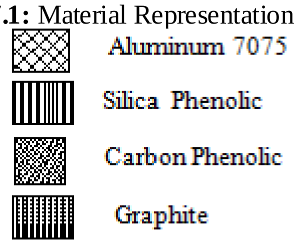

7.2 Structural analysis

7.2.1 Finite element analysis: (in ansys)

Finite element analysis of the nozzle assembly package. Following area unit the steps concerned within the analysis.

Step-1: Import 2D model from AutoCAD through IGES format.
Step-2: Analysis Type: Structural
Element Type: Solid, 8 node 82
Step-3: Specify material properties as mentioned within the table.

Material	Young's modulus	Poisson's ratio	Ultimate tensile Strength
Aluminum 7075	7378	0.33	42.9
Silica Phenolic	1700	0.28	9
Carbon Phenolic	900	0.25	10
Graphite	1180	0.3	10.5

Step-4: Crete different areas
Step-5: Assign material properties to the different areas
Step-6: Mesh
Free mesh with the element edge length of 0.5 accuracy

Figure 7.1: Crete different areas

Step-7: Define loads

Apply constant pressure of 1 atm as shown in the figure

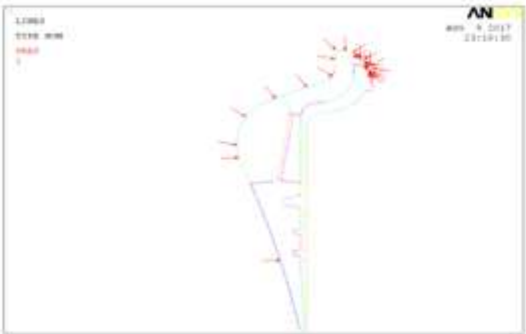

Figure 7.2: As per on the nodes when pressure is applied it is as shown in the figure.

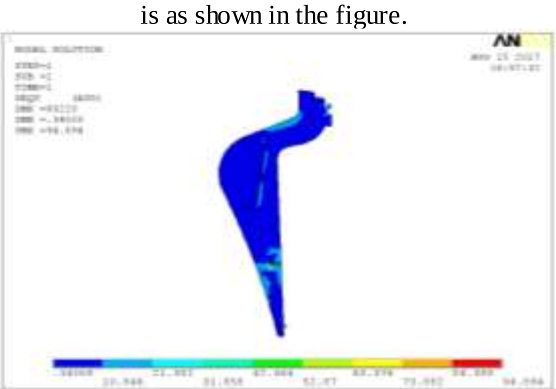

Figure 7.3: Free mesh with the element edge length of 0.5 accuracy

Step-8: Solve the problem (solve – Current LS)
Step-9: Check the results, Stress – Von Misses Stress

MESH:
The following figures show the mesh for finishing up the analysis. Element selected for analysis plane 82 (8 nodded quadrature element) with element size factor 1.

Figure 7.4: Formation of the elements after mesh

Boundary Conditions
Pressure of 1.0 kg/mm2 is applied on Nozzle casing at oblique entry until O ring, and variable internal pressure is applied on nozzle contour.

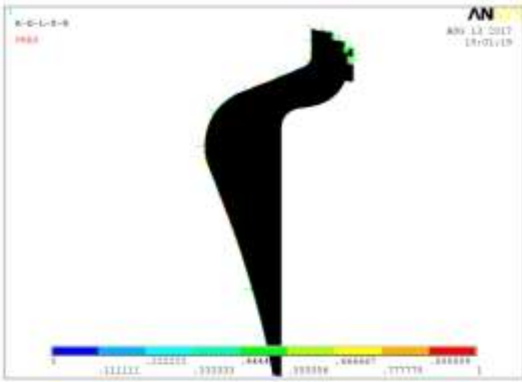

Figure 7.5: as per on the nodes when pressure is applied

8. Results

The von misses stresses on various components with FOS are given in table. The Von Misses stress at different interfaces is shown in the figures.

Stresses in various region

Location	Vonmises Stress (kg/mm^2)	FOS
In the Nozzle casing	22.51	4.21
In the graphite throat	1.66	6.32
at the nozzle convergent entry	2.2	4
At nozzle convergent to straight portion	1.0	10.5

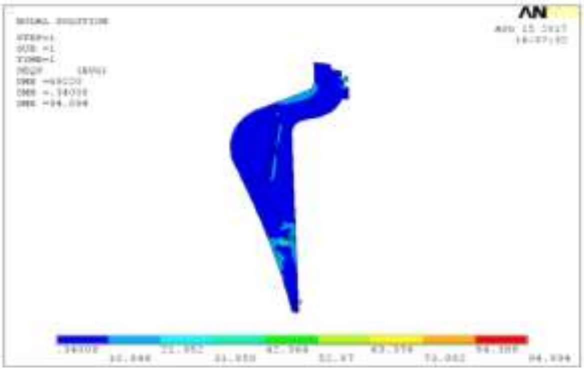

Figure 7.6: Von Misses stress distribution on the Nozzle assembly

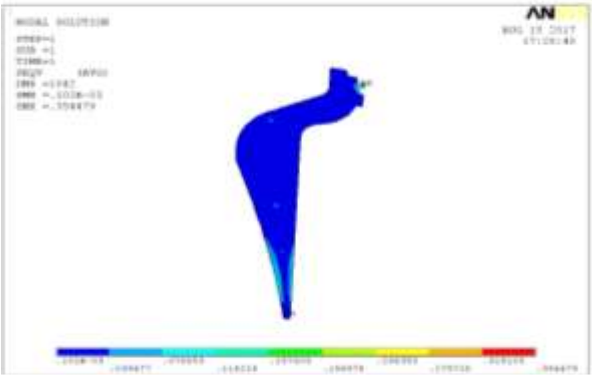

Figure 7.7: Deflection in the Nozzle assembly

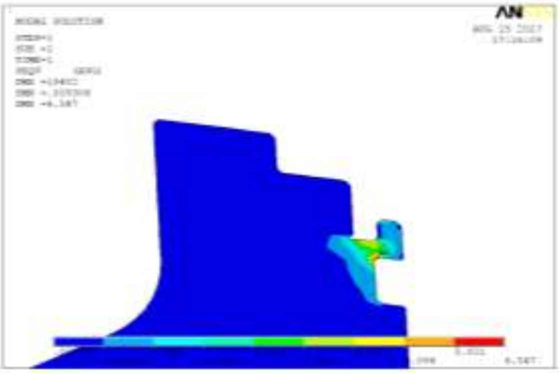

Figure 7.8: Von Misses stress on the Nozzle assembly (show maximum value)

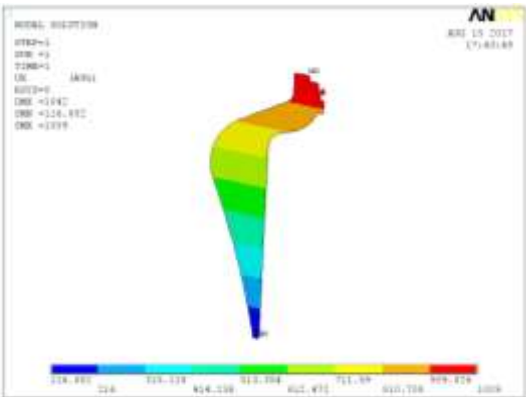

Figure 7.9: Deflection in X and Y direction in nozzle casing

From the figure, it is clear that the maximum von misses stress is about 94.89 kg/mm^{2}is acting over small region hence neglected. The stress of 22.51kg/mm^2 have been consider for FOS calculations. The UTS of the AA 7075 has been thought of as 94.83 kg/mm^2 .By considering 22.51 kg/mm2 to be the utmost stress the FOS accessible on UTS is 1.9.

9. Results and Discussions

8.1 Results and Discussions of case design

By the GVR Rao method approximation method, we have designed the contour of nozzle. Gives the parabolic contour of the inner wall of the nozzle, these calculations were carried out by using the formulae discussed in the chapter 5.

8.2 Results and Discussions of thermal analysis

In the thermal analysis of the nozzle, the heat transfer to the wall of due to the flow inside the nozzle from inlet to exit is calculated by using Bartz equation. Graphite insert is used as it undergoes ablative burning and protects the remaining parts of the nozzle.

8.3 Results and Discussions of structural analysis

The structural analysis is carried out by using ANSYS Mechanical APDL. The stress generated is calculated by elaboration Von-Misses Stress. The pressure values are calculated by using isentropic flow relations. The pressure at the water is most and also the pressure at the exit is minimum. The pressure values can be obtained from the plot-6.4. The displacement values obtained are 6.8mm, the maximum and minimum stress is 1241. 86 and -0.2745×10-10 the results and distorted and distorted shapes are shown in figure below. In the structural analysis, the force excreted on the graphite insert is also calculated as 11657.71kgs. The results have been showed below.

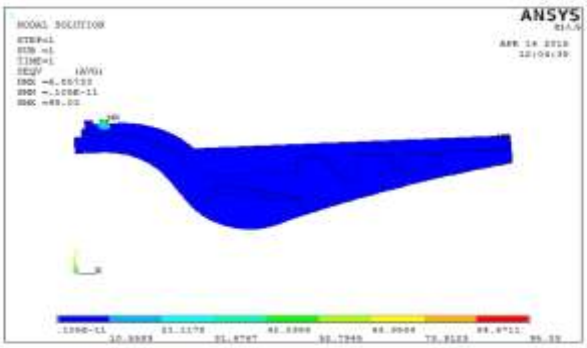

Figure 8.1: Von Misses Stress

Figure 8.2: Deflection

10. Conclusions

The project work aimed at designing the nozzle contour in order to produce a required amount of thrust was successfully obtained. All the designing methods the G.V.R. Rao approximation method is best and simplest method.

A MATLAB program has been defined the coordinates. These coordinates help us to design a nozzle in CAD software. After obtaining the contour profile, calculation of the liner thickness was carried out. Liners facilitate the walls of the nozzle to face up to the warmth flux created throughout the combustion method.

It has been recognized that the combustion gases to the walls of each combustion chamber and therefore the nozzle. Therefore, the thermal analysis of the rocket nozzle consisted of the calculation of the warmth transfer co-efficient on the length of the nozzle ranging from the water to the exit of the nozzle, which was helpful in selecting components that is to be placed in warm temperature region and that one within the coldness regions.

To get a structurally stable style, structural analysis was dole out by applying pressure on the wall of the contour. This analysis helped us to know that whether the designed structure can withstand the applied pressure that was applied.

References

[1] George P. Sutton and Oscar Biblarz, "Rocket Propulsion Elements" A Wiley-Interscience Publication, 7 th edition, PP 21-23, PP24-33
[2] M. Barrere, A. Jaumotte, B. Fraeijs De Veubeke, and J. Vandenkerckhove, "Rocket Propulsion", Elsevier Publishing Company, Amsterdam, 1960, PP 9-21
[3] G.V.R. Rao, Exhaust Nozzle Contour for Optimization thrust, jet propulsion, June, 1958, PP 34-38, PP 40-42
[4] D.R. Bartz, "Turbulent Boundary Layer Heat Transfer from Rapidly Accelerating Flow of Rocket Combustion Gases and of Heated Air", Jet Propulsion Laboratory, Page no. 43-44
[5] Konstantin A. Kurbatskii1 and Angela Lestari2, "Pressure-based Coupled Numerical Approach to the Problem of Compressible Flow through Convergent Conical Nozzles" ANSYS Inc., Lebanon, NH 03766, USA, PP 8
[6] G. V. R. Rao, J. E. Beck, and T. E. Booth, Boeing/Rocketdyne Propulsion & Power Canoga Park, CA, "Nozzle Optimization for Space-Based Vehicles", AIAA 99-2584, PP 11
[7] John Mern and Ramesh Agarwal, "A Study of Numerical Simulation of Supersonic Conical Nozzle Exhaust" Department of Mechanical Engineering and Materials Science Washington University in St. Louis, 1 Brookings Drive, St. Louis, MO 63130, PP 8
[8] G. V. R. Rao, Rocketdyne Division Rockwell International Corporation Canoga Park, CA and A. L. Dang Physical Research Inc. Irvine, CAAI, "Thrust Optimization of Nozzle Contour Including Finite Rate Chemical Kinetics", AIAA 92-3729, PP 11
[9] http://en.wikipedia.org/wiki/Rocket_engine_nozzle, PP 1-6.